

# Anion Receptors Based on Halogen Bonding with Halo-1,2,3-triazoliums

Ronny Tepper,<sup>†,‡</sup> Benjamin Schulze,<sup>†,‡</sup> Michael Jäger,<sup>†,‡</sup> Christian Friebe,<sup>†,‡</sup> Daniel H. Scharf,<sup>§</sup> Helmar Görls,<sup>||</sup> and Ulrich S. Schubert<sup>\*,†,‡</sup>

<sup>†</sup>Laboratory of Organic and Macromolecular Chemistry (IOMC), Friedrich Schiller University Jena, Humboldtstr. 10, 07743 Jena, Germany

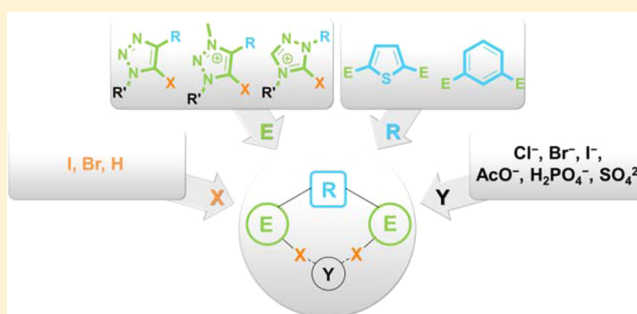
<sup>‡</sup>Jena Center for Soft Matters (JCSM), Friedrich Schiller University Jena, Philosophenweg 7, 07743 Jena, Germany

<sup>§</sup>Leibniz Institute for Natural Product Research and Infection Biology – Hans Knöll Institute, Beutenbergstr. 11a, 07745 Jena, Germany

<sup>||</sup>Laboratory of Inorganic and Analytical Chemistry, Friedrich Schiller University Jena, Lessingstr. 8, 07743 Jena, Germany

## Supporting Information

**ABSTRACT:** A systematic series of anion receptors based on bidentate halogen bonding by halo-triazoles and -triazoliums is presented. The influence of the halogen bond donor atom, the electron-withdrawing group, and the linker group that bridges the two donor moieties is investigated. Additionally, a comparison with hydrogen bond-based analogues is provided. A new, efficient synthetic approach to introduce different halogens into the heterocycles is established using silver(I)-triazolylidenes, which are converted to the corresponding halo-1,2,3-triazoliums with different halogens. Comprehensive nuclear magnetic resonance binding studies supported by isothermal titration calorimetry studies were performed with different halides and oxo-anions to evaluate the influence of key parameters of the halogen bond donor, namely, polarization of the halogen and the bond angle to the anion. The results show a larger anion affinity in the case of more charge-dense halides as well as a general preference of the receptors to bind oxo-anions, in particular sulfate, over halides.



## INTRODUCTION

Owing to the importance of anions in biological and chemical processes, considerable research efforts have been devoted to the design of selective anion binding sites.<sup>1</sup> Although anion detection based on hydrogen bonds, ion–ion, Lewis acid–base, and anion– $\pi$  interactions has been intensively studied,<sup>2–4</sup> the potential of (charge-assisted) halogen bonds<sup>5</sup> for selective anion recognition was realized only recently.<sup>6,7</sup> Subsequently, comprehensive studies have shown great potential of the halogen bond for the application in anion sensing,<sup>8,9</sup> organo-catalysis,<sup>10–20</sup> and anion-templated construction of interlocked structures.<sup>8,21–26</sup>

Halogen bonds are supramolecular interactions between a Lewis base (Y) and a Lewis-acidic region ( $\sigma$  hole<sup>27</sup>) of a covalently bound halogen (X).<sup>5,27–30</sup> This region of positive electrostatic potential is the result of an electron-density displacement upon bond formation between X and an electron-withdrawing group (E) and is thus located on the opposite end of the E–X bond. The size of the  $\sigma$  hole and, consequently, the strength of the halogen bond depends on the effective electronegativity of E as well as on the polarizability of X with the latter increasing in the order Cl < Br < I.<sup>27,28,30</sup> The halogen bond features a strong preference for a bond angle

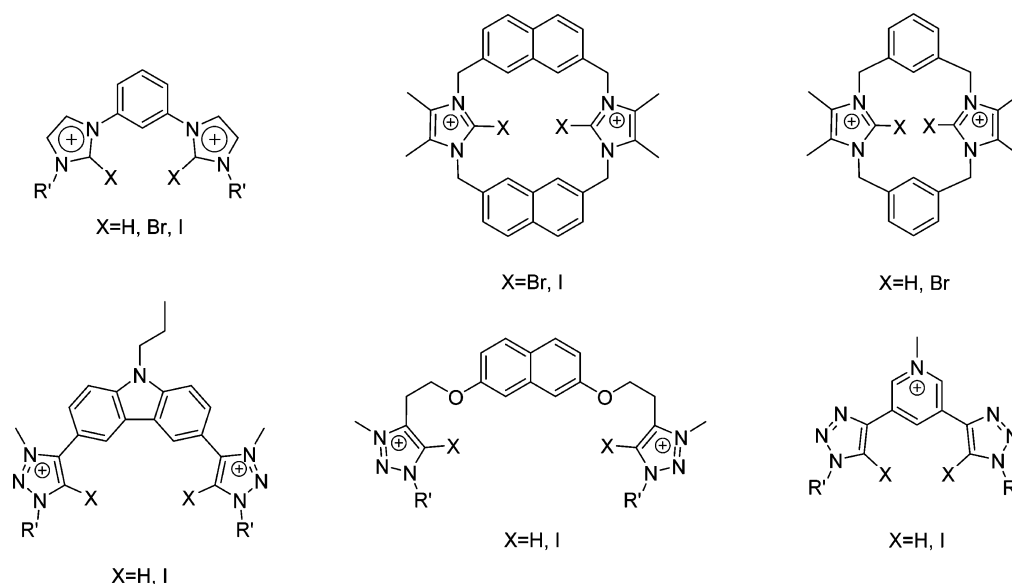
(E–X...Y) close to 180° in order to minimize electronic repulsion with the electron-rich belt surrounding the hole.<sup>31,32</sup> This orientational preference is much more pronounced than that for the analogous hydrogen bond, which gives rise to the construction of highly directional and selective anion binding sites. Another advantage of halogen bond-based systems is their ability to bind also soft anions, such as iodide, very effectively, which is tentatively assigned to a larger covalent contribution toward the halogen bond interactions.<sup>26,29,33</sup>

To date, neutral systems based on perfluoroiodo arenes<sup>31,33,37–42</sup> and cationic halo-imidazolium systems<sup>8,9,13,33,34,36,43,44</sup> have been established as halogen bond donors. Recently, it was demonstrated that the nitrogen-rich 1,2,3-triazole and -triazolium systems feature strongly polarized C–H/C–X bonds, which enable strong (charge-assisted) hydrogen/halogen bonds.<sup>29</sup> Although halide abstraction with 1,3-bis(iodo-1,2,3-triazolium)benzene receptors<sup>14</sup> and the anion affinity of several iodo-1,2,3-triazolium-based receptors<sup>21,22,24,25,32,35,45,46</sup> have been reported, a systematic anion binding study on rigid cleft-type receptors featuring halo-1,2,3-

Received: January 9, 2015

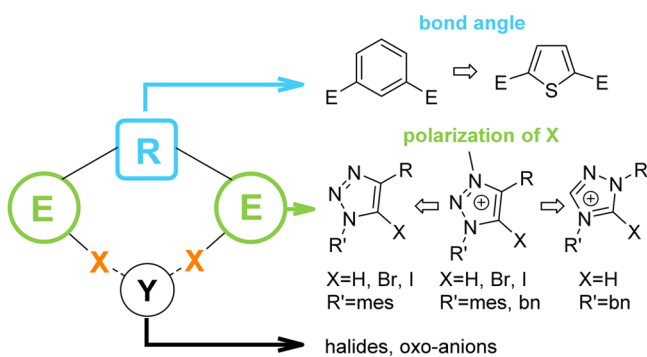
Published: February 11, 2015

Scheme 1. Schematic Representation of Charged Bidentate Halogen Bond Receptors For Which Anion Affinities Were Quantified in Former Studies<sup>9,25,26,34–36</sup>



triazoliums has been absent to date. Even on structurally related bidentate receptors, only a few detailed binding studies have been reported (Scheme 1).<sup>9,32–34</sup> Therefore, we study herein the effect of each tunable property of cleft-type halogen bond donors, namely, the polarization of X, the bond angle to the anion, and the influence of the anion itself (Scheme 2). We

Scheme 2. Schematic Representation of the Systematic Variation of the Receptors in the Presented Survey



were interested in further developing anion receptors based on halo-1,2,3-triazoles and -triazoliums owing to their facile and modular synthesis via copper(I)-catalyzed azide–alkyne cycloaddition (CuAAC).<sup>29,47,50</sup> For comparison, hydrogen-bond analogues and 1,2,4-triazole analogous receptors were also synthesized and investigated.

## RESULTS AND DISCUSSION

**Synthesis.** The 1,2,3-triazole moiety can be obtained through the facile and modular CuAAC reaction (Scheme 3).<sup>29,47,48,51</sup> With this method, cleft-type hydrogen bond donors like 1,3-bis(1,2,3-triazol-4-yl)benzene **1** (Scheme 4a) can be readily prepared.<sup>52,53</sup> To synthesize the corresponding halogen bond donors, the relatively high C–H acidity in the 5-position of the 1,2,3-triazole ( $pK_a = 28$ )<sup>29</sup> can be exploited. Accordingly, regioselective metalation by *n*-BuLi and the subsequent treatment with iodine afforded 5-iodo-1,2,3-triazole-based

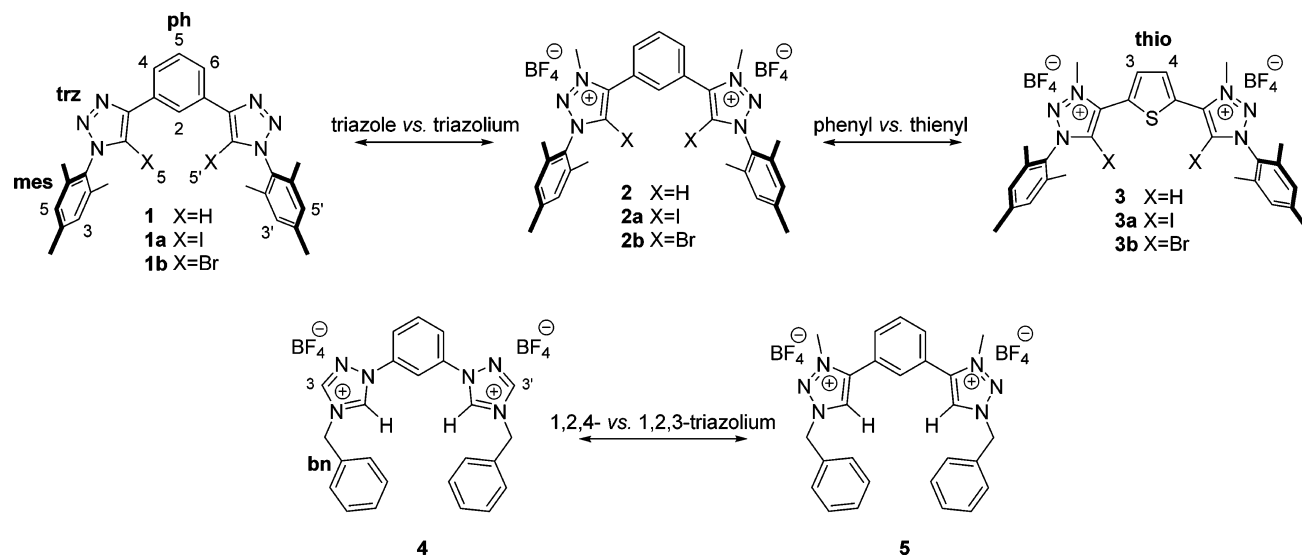
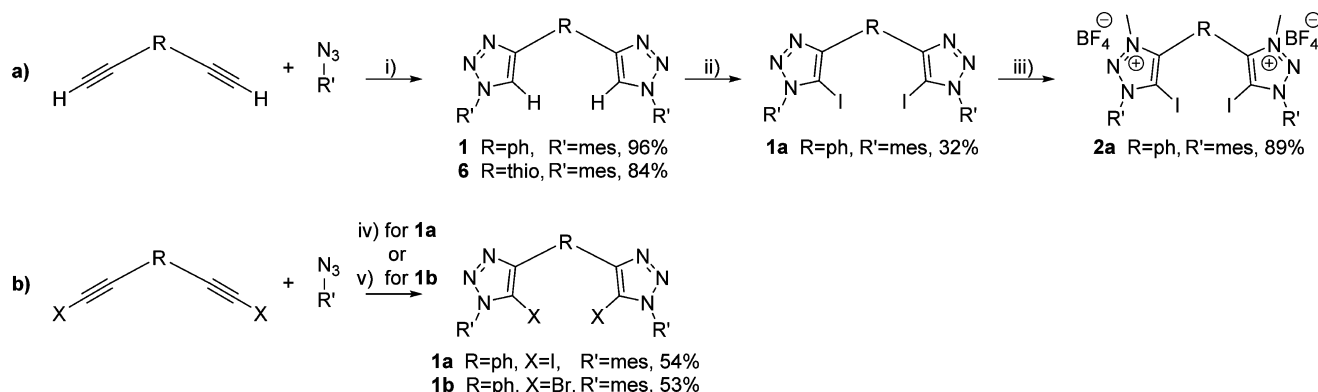
receptor **1a** (Scheme 4a);<sup>54</sup> however, the yield was only modest (32%) and the analogous reaction with bromine to obtain **1b** failed. Thus, 5-halo-1,2,3-triazoles were prepared via an alternative route by a copper(I)-catalyzed cycloaddition between halo-alkynes and azides.<sup>14,55–58</sup> For instance, **1a** was obtained using 1,3-bis(iodoethyl)benzene in moderate yields (54%) following a previously reported procedure.<sup>14</sup> More importantly, 1,3-bis(bromoethyl)benzene<sup>59</sup> gave **1b** in only one step (Scheme 4b)<sup>56</sup> with comparable yields (53%); however, very long reaction times were required.

To enhance the C–H/C–X bond polarization and to increase anion affinity via additional Coulomb interactions with the anions, the 1,2,3-triazoles can be alkylated (e.g., using trimethyloxonium tetrafluoroborate),<sup>21,53,60</sup> which is exemplified for **2a** (Scheme 4a).<sup>29</sup> However, as halogen installation at the 1,2,3-triazole precursor is less efficient (vide supra), we were also interested in developing a more general approach toward halo-1,2,3-triazoliums. Accordingly, we anticipated that silver(I)-1,2,3-triazolylidenes, which can be prepared conveniently by metalation of 1,2,3-triazoliums using  $Ag_2O$ ,<sup>29,61–63</sup> might be converted to the corresponding halo-1,2,3-triazoliums with different halogens. Indeed, driven by precipitation of the corresponding silver(I)-halides, 5-iodo- (**3a**) and 5-bromo-1,2,3-triazoliums (**2b** and **3b**) were obtained in very good yields (86–93%) after treatment of the silver(I)-carbene complex with iodine or bromine (Scheme 5).

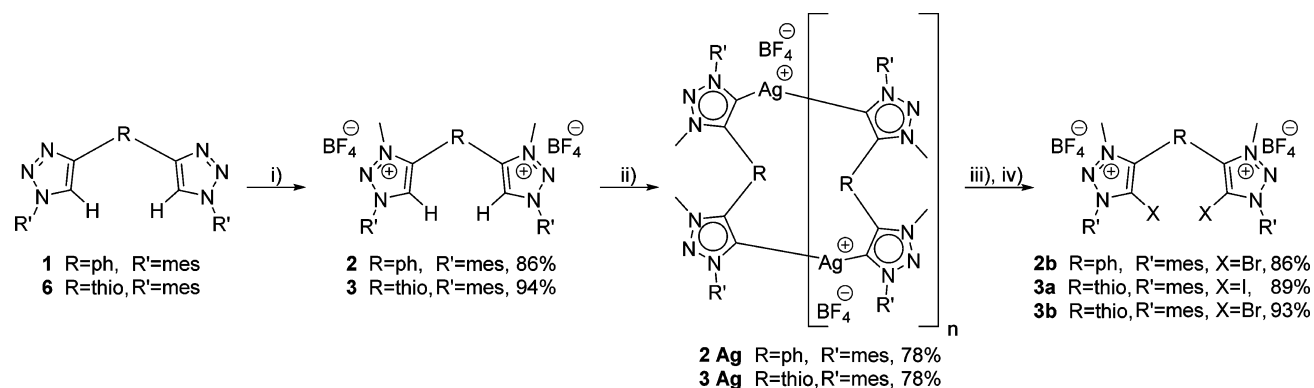
To ensure the uniformity of the counterion for subsequent binding studies, the product was repeatedly washed with an aqueous ammonium tetrafluoroborate solution, and the identity and purity of the product was confirmed by NMR, MS, and elemental analysis. Importantly, this improved route enables the facile synthesis of 1,2,3-triazoliums via CuAAC and subsequent methylation as well as the efficient introduction of iodine and even bromine at the final stage.

For comparison, receptors based on the 1,2,4-triazolium fragment as polarizing group E were also synthesized. The hydrogen-bond reference system **4** was obtained following a literature procedure<sup>64,65</sup> and subsequent counterion exchange. The corresponding silver(I)-1,2,4-triazolylidene complex **4Ag**

Scheme 3. Schematic Representation of the Investigated Receptors

Scheme 4. Schematic Representation of the Synthesis of Receptors 1, 1a, 1b, and 2a<sup>a</sup>

<sup>a</sup>(i)  $\text{CuSO}_4$ , NaAsc., EtOH/H<sub>2</sub>O/CH<sub>2</sub>Cl<sub>2</sub> (2:1:1), 50 °C; (ii) *n*-BuLi, THF, -78 °C, I<sub>2</sub>; (iii) Me<sub>3</sub>OBF<sub>4</sub>, CH<sub>2</sub>Cl<sub>2</sub>, room temperature (rt), 3 d; (iv) CuI/TBTA, THF, rt, 6 d; and (v) CuBr/CuAcO, THF, 50 °C, 14 d.

Scheme 5. Schematic Representation of the Synthesis of Receptors 2, 2b, 3, 3a, and 3b<sup>a</sup>

<sup>a</sup>(i) Me<sub>3</sub>OBF<sub>4</sub>, CH<sub>2</sub>Cl<sub>2</sub>, rt, 1–3 d; (ii) Ag<sub>2</sub>O, molecular sieves, MeCN, reflux, 12 h; (iii) X<sub>2</sub> at 0 °C for 30 min, then rt for 1 h; and (iv) 1 M NH<sub>4</sub>BF<sub>4(aq)</sub> for anion exchange.

was synthesized<sup>64</sup> in good yield (88%), and regioselective deprotonation in the 5-position was proven by <sup>1</sup>H NMR spectroscopy. However, after treatment of the silver(I)-complex with iodine as described above, the 5-iodo-1,2,4-triazolium system could not be isolated. As revealed by NMR spectroscopy

and single-crystal X-ray diffraction, only the hydrogen-bond system 4 and a mesoionic 1,2,4-triazolium-5-oxide<sup>66</sup> (Figure S57a, Supporting Information (SI)) were obtained. On the other hand, when using bromine, a partially decomposed product could be isolated and characterized crystallographically

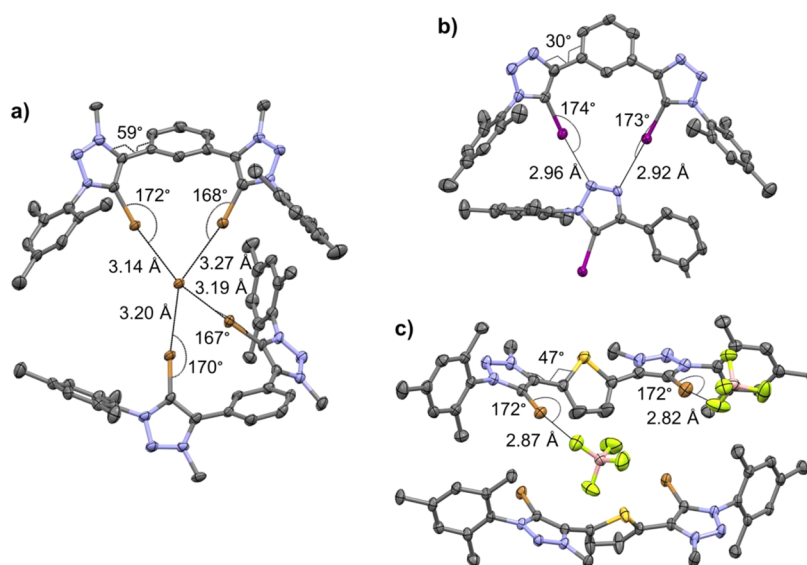


**Figure 1.** Molecular structures of (a) **2b**, (b) **1a**, and (c) **3b** (thermal ellipsoids at 50% probability level, hydrogen atoms, counterions, solvent molecules, and errors for the discussed values are omitted for clarity; see Figure S61, SI). Errors have no influence on the reliability of the discussed trends; gray, carbon; blue, nitrogen; purple, iodine; yellow, sulfur; green, fluorine; pink, boron; and brown, bromide.

(Figure S57b, SI). Although the quality of the single crystals was too low to discuss structural parameters, a C–Br⋯Br<sup>−</sup> halogen bond involving one of the 1,2,4-triazolium moieties was unambiguously confirmed. Seemingly, the C–X polarization in the case of the 1,2,4-triazolium fragment is too high, resulting in C–I cleavage upon halogen bond formation (similar to *N*-iodosuccinimide).<sup>6,67</sup> In contrast, the C–Br bond is less polarized and thus less reactive.

Note that the 1,2,4-triazolium receptor was benzyl-functionalized for synthetic ease<sup>64</sup> and, to ensure comparability between the 1,2,3- and 1,2,4-triazolium-based systems, a benzyl-functionalized 1,2,3-triazolium reference system **5** was synthesized as well.<sup>68,69</sup>

**Crystal Structures.** Single crystals of several receptors could be grown by slow vapor diffusion of different nonsolvents into a concentrated solution (Figure 1). In all cases, the intended binding site is readily accessible for anions as the mesityl groups (R') are arranged orthogonally to the 1,2,3-triazoles. Additionally, this twisted structure inhibits intermolecular  $\pi$ -stacking thereby increasing the solubility of the receptors.

Initial attempts to crystallize **2b** (Figure 1a) prior to anion exchange (*vide supra*) revealed a 2:1 complex with bromide, which is ascribed to an excess of the receptor with respect to the anion. Two receptors form four nearly linear halogen bonds (167–172°) with a single bromide, which is coordinated in a distorted tetrahedral fashion. To enable this highly directed interaction in a bis-bidentate fashion, the triazolium rings twist out of the plane of the central phenyl ring by 59°. The measured halogen bond lengths range from 3.14 to 3.27 Å, which is significantly shorter than the sum of the van der Waals radii (3.70 Å)<sup>70</sup> and comparable to related complexes.<sup>9,71,72</sup>

In the case of **1a** (Figure 1b), a dimer formed by two nearly linear halogen bonds (173°–174°) between the iodines and two different nitrogen atoms of a single triazole ring could be observed. This clearly demonstrates already that the uncharged iodo-1,2,3-triazole exhibits C–I bond polarization suitable for halogen bond formation.<sup>55</sup> In contrast, the corresponding bromo-substituted receptor **1b** does not show any halogen

bond interactions in the solid state (see Figure S58, SI), which is ascribed to the lower polarizability of the halogen bond-donor atom. Furthermore, the triazoles and the central phenyl ring adopt a smaller dihedral angle (30°), which is attributed to the absence of sterically demanding 1,2,3-triazolium methyl groups and binding toward two contiguous nitrogen atoms.

Figure 1c shows two individual monodentate halogen bonds with the two counterions in the case of **3b**, which is presumably the result of electronic and steric repulsion between the sulfur and the halogen atoms. Additionally, anion– $\pi$  interactions involving the 1,2,3-triazoliums are observed in the solid state.

Furthermore, single crystals of a sulfate complex were grown by carefully layering concentrated acetonitrile solutions of **2a** and (NBu<sub>4</sub>)<sub>2</sub>SO<sub>4</sub> (Figure 2). X-ray diffraction reveals bidentate

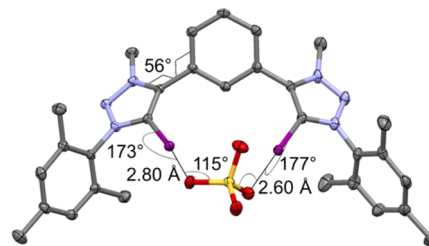


**Figure 2.** Molecular structure of **2a** interacting with sulfate (thermal ellipsoids at 50% probability level, hydrogen atoms, solvent molecules, boronic acid, and errors for the discussed values are omitted for clarity; see Figure S62, SI). Errors have no influence on the reliability of the discussed trends; gray, carbon; blue, nitrogen; purple, iodine; yellow, sulfur; and red, oxygen).

complexation of a single sulfate anion via two different oxygen atoms in the solid state. Notably, a boronic acid molecule also binds to the sulfate, which is presumably formed by hydrolysis of the original tetrafluoroborate counterions of **2a** (see Figure S60, SI). As a result, different C–I⋯O bond lengths of 2.80 and 2.60 Å were observed.<sup>72</sup> Both halogen bonds are close to linearity and are significantly shorter than the sum of the van der Waals radii (3.50 Å).<sup>70</sup> Aside from a very recently published catenane–sulfate complex,<sup>26</sup> this is the only crystallographic

report of a halogen bond-based sulfate complex reported to date. Although the boronic acid adduct as well as packing effects may in principle lead to a preference for this binding mode, bidentate halogen bonding with two different oxygen atoms of the sulfate is also the preferential complexation mode according to DFT modeling (see Figure S64, SI).

**Binding Studies.** NMR studies (Table 1) as well as isothermal titration calorimetry (ITC) measurements (Table 2)

**Table 1. Overview of NMR Titration Data for Various Receptors with Different Anions**

	E-X	Y	solvent	$K_1$ [ $M^{-1}$ ] <sup>a</sup>	$K_2$ [ $M^{-1}$ ] <sup>a</sup>	
triazolium reference system	2a	I <sup>-</sup>	DMSO	670 ( $\pm 30$ )	<15	
		Br <sup>-</sup>	DMSO	860 ( $\pm 30$ )	<15	
		Cl <sup>-</sup>	DMSO	1200 ( $\pm 30$ )	<15	
		AcO <sup>-</sup>	DMSO	1740 ( $\pm 40$ )	<15	
		H <sub>2</sub> PO <sub>4</sub> <sup>-</sup>	DMSO	2310 ( $\pm 40$ )	<15	
triazole bond donor	1a	Cl <sup>-</sup>	DMSO	51 ( $\pm 1$ )	<15	
						2b
H-analogues	2	Cl <sup>-</sup>	DMSO	104 ( $\pm 3$ )	<15	
				5	99 ( $\pm 2$ ) <sup>b</sup>	<15 <sup>b</sup>
				4	89 ( $\pm 3$ ) <sup>b</sup>	<15 <sup>b</sup>
linker R	3a	I <sup>-</sup>	DMSO	90 ( $\pm 2$ )	<15	
				Br <sup>-</sup>	DMSO	170 ( $\pm 30$ )
		3b	Cl <sup>-</sup>	DMSO	298 ( $\pm 8$ )	<15
					85 ( $\pm 1$ )	<15

<sup>a</sup>Association constants and errors calculated using WinEQNMR2 and *H*-3,5<sup>mes</sup> chemical shifts. <sup>b</sup>Association constants and errors calculated using WinEQNMR2 and *H*-5<sup>trz</sup> chemical shifts.

were performed to quantify the influence of the various receptor components (E, R, and X). Because the formed complexes precipitated during the NMR titration in MeCN, the NMR studies had to be performed with a more competitive solvent (DMSO). In contrast, due to the lower concentrations required for ITC studies, no solubility issues were encountered in MeCN, whereas no heat effect was observed in DMSO.<sup>34</sup> Evaluation of the NMR titration data was accomplished with the help of WinEQNMR2 software.<sup>73</sup> Because the mesityl moiety is present in most of the receptors and the proton resonances of the central phenyl spacer overlap in some cases (see Figure S39, SI), the *H*-3,5<sup>mes</sup> shift migration was used for determining the binding constants.

**Table 2. Overview of ITC Titration Results for Various Receptors with Different Bu<sub>4</sub>N<sup>+</sup> Anions**

	E-X	Y	solvent	model (step <i>n</i> )	$K_n$ [ $M^{-1}$ ]	$\Delta G$ [ $kJ mol^{-1}$ ]	$\Delta H$ [ $kJ mol^{-1}$ ]	T $\Delta S$ [ $kJ mol^{-1}$ ]	$N_n$
bond acceptor	2a	I <sup>-</sup>	MeCN	OneSites	$8.35 \times 10^4$	-25.1	-17.7	7.4	0.89
				TwoSites (1)	$3.22 \times 10^5$	-31.9	-16.4	15.5	0.90
		Br <sup>-</sup>	MeCN	TwoSites (2)	$1.21 \times 10^3$	-18.0	-3.5	14.5	0.83
				Cl <sup>-</sup>	MeCN	TwoSites (1)	$4.75 \times 10^5$	-32.9	-14.4
bond donor	2	Cl <sup>-</sup>	MeCN	TwoSites (2)	$1.78 \times 10^3$	-18.9	-7.2	11.7	0.83
				OneSites	$9.76 \times 10^2$	-17.4	-9.6	7.8	0.80
linker R	3a	Cl <sup>-</sup>	MeCN	<i>a</i>	$7.26 \times 10^3$	-22.4	-11.9	10.5	1.42

<sup>a</sup>No heat effect was observed in the ITC measurements.

**NMR Studies.** The phenyl-based iodo-1,2,3-triazolium system 2a was selected as a reference. In Figure 3 (top), a

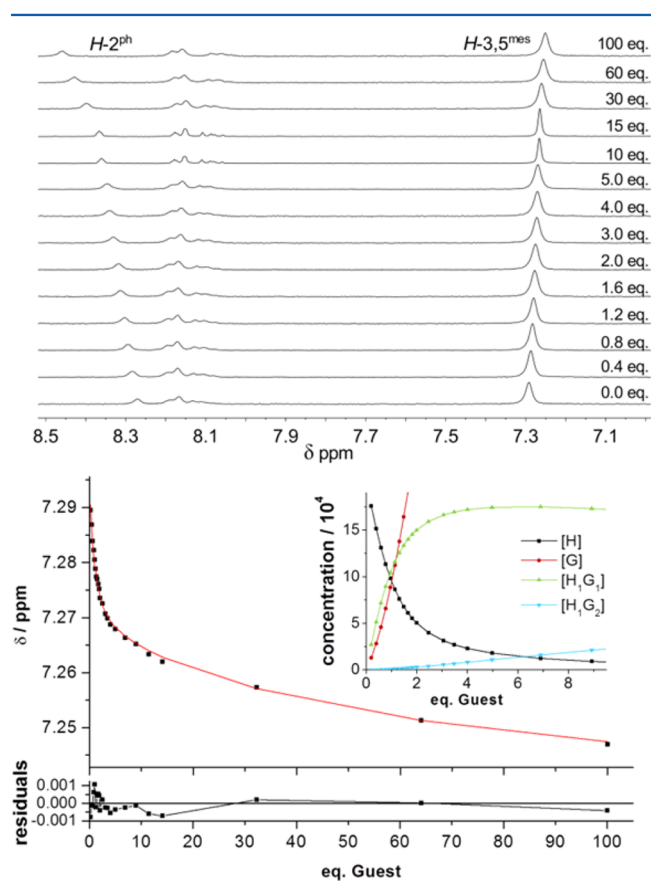


**Figure 3.** (Top) Partial <sup>1</sup>H NMR spectra of receptor 2a upon the addition of Bu<sub>4</sub>N<sup>+</sup>Cl<sup>-</sup> (300 MHz, DMSO-*d*<sub>6</sub>). (Bottom) Obtained fit curve (red line) and residuals for this titration assuming a 1:2 complex (calculated using *H*-3,5<sup>mes</sup> chemical shifts), and (inset) speciation curves for all of the involved species (H = host, G = guest).

typical chemical-shift migration obtained by the titration of 2a with a tetra-*n*-butylammonium (Bu<sub>4</sub>N<sup>+</sup>) halide is depicted. Upon titration, a downfield shift of the *H*-2<sup>ph</sup> signal and a less pronounced highfield shift for the *H*-3,5<sup>mes</sup> signal is observed with the latter being ascribed to anion- $\pi$  interactions.<sup>74</sup> In line with the maximum at 0.5 in the corresponding Job plot (see Figure S33, SI), evaluation of the binding isotherm<sup>75</sup> suggests the predominant formation of a 1:1 complex accompanied by the formation of a weak 1:2 host-guest complex (Table 1). This behavior and the substantially larger  $K_1$  value relative to similar monodentate halogen bond donors ( $\sim 10^2 M^{-1}$ )<sup>43</sup>

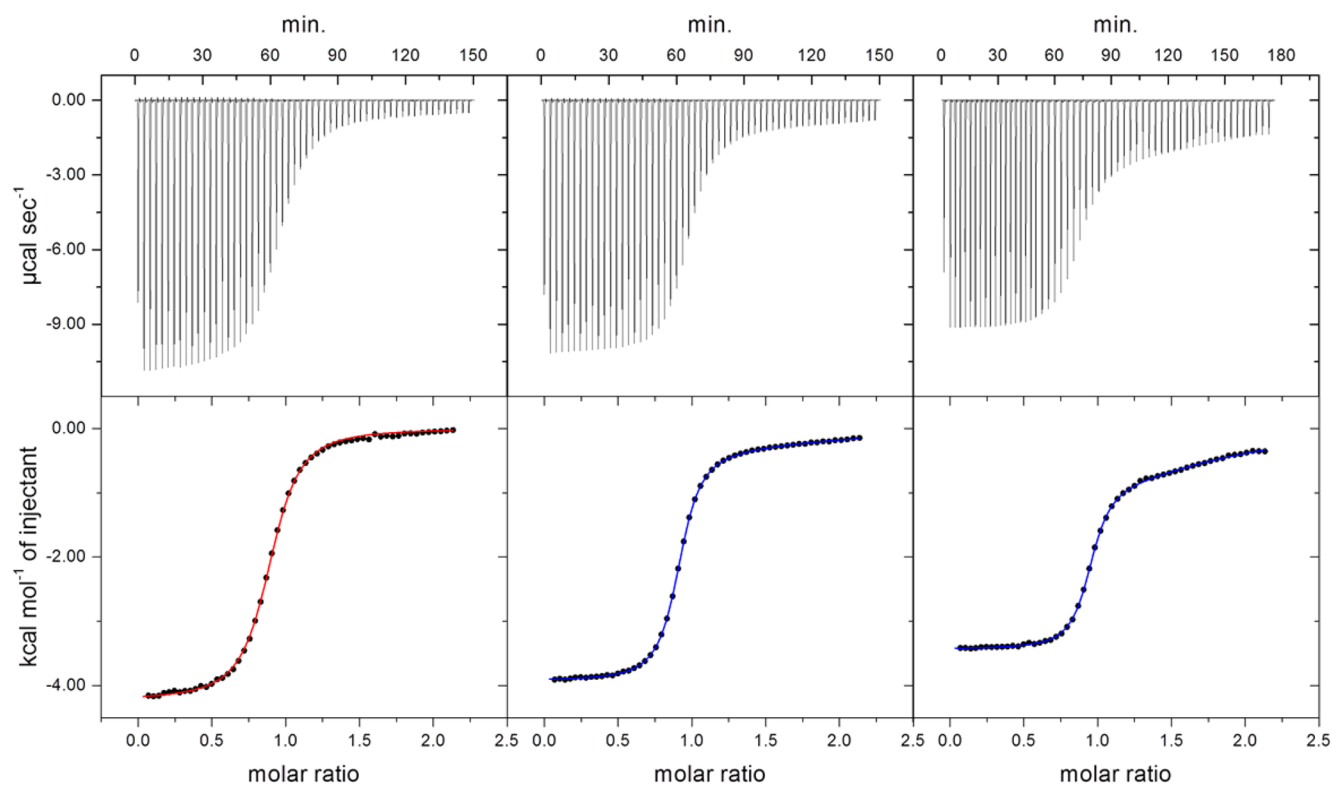


**Figure 4.** ITC evaluation of  $2a \cdot I^-$  (left),  $2a \cdot Br^-$  (middle), and  $2a \cdot Cl^-$  (right) using two different fitting models (OneSites = red, TwoSites = blue, for detailed experimental information see Table S1, SI).

strongly suggest a preferential bidentate binding mode. The assumption of a 1:2 complex is required to explain the minor chemical-shift perturbations upon the addition of 10–100 equiv, which implies that the second complexation step only becomes relevant if an excess of guest is provided (see the speciation curve in Figure 3, bottom). The trend for the  $K_1$  values (Table 1) shows a general preference for more charge-dense/basic halides as the bond acceptor ( $Cl^- > Br^- > I^-$ ), which allows for a stronger electrostatic as well as charge-transfer interaction. Nevertheless, the soft halides are also strongly bound, which is tentatively assigned to a larger covalent contribution toward the halogen bond interactions compared to that of the analogous hydrogen bond systems.<sup>29,33</sup>

In comparison to the halides, the complexation of acetate, dihydrogen phosphate, and sulfate is much stronger, which was also found previously in analogous studies<sup>43</sup> and is rationalized by the higher basicity of the selected oxo-anions. The observed slight preference for dihydrogen phosphate over acetate is contrary to the higher charge density and basicity of acetate and is thus ascribed to a better fit between the receptor's cavity and the tetrahedral anion. The observation of the highest anion affinity in the case of sulfate is rationalized by its doubly negative charge, which provides a significantly enhanced charge assistance.<sup>29,53,76</sup>

In comparison with the iodo-1,2,3-triazolium receptor **2a**, the bromo analogue **2b** revealed a significantly lower halide affinity (Table 1) in line with the lower polarizability of the bromine atom. Like **2a**, the NMR data shows a preference of **2b** for more charge-dense halides ( $Cl^- > Br^- > I^-$ ).

Dependence of the interaction strength on the electron-withdrawing group is also apparent from Table 1. Although the individual contributions of charge assistance and increased polarization cannot be distinguished, comparison of triazole-

and a triazolium-containing receptors (**1a** vs **2a**) clearly demonstrates the superior chloride affinity of the iodo-triazolium system. As the chloride affinity of **1a** is already at the lower limit of detectable interactions, NMR titrations with bromide and iodide as well as binding studies for receptor **1b** were omitted.

As halogen introduction for 1,2,4-triazoliums failed (vide supra), the electron-withdrawing character was studied by comparing the benzyl-equipped 1,2,4- and 1,2,3-triazolium-based hydrogen bond donors **4** and **5**. According to the significantly higher chloride affinity of **4** (Table 1), the electron-withdrawing character of the 1,2,4-triazolium moiety is superior to that of 1,2,3-triazolium (vide infra).<sup>29</sup> Additionally, a comparison between the 1,2,3-triazolium receptors **2** and **5** showed a marginally lower anion affinity in the case of the latter (Table 1), which is in line with the weaker electron-withdrawing character of the benzyl substituent relative to that of an aryl group.<sup>29</sup>

Finally, the bidentate halo-1,2,3-triazolium receptors featuring phenyl and thienyl spacers were compared. Relative to **2a**, the halide affinity of **3a** is significantly lower, although the same halide preference ( $Cl^- > Br^- > I^-$ ) was observed. The combination of bromo-1,2,3-triazolium and a thienyl spacer (**3b**) leads to even weaker chloride binding than that of both **3a** and **2b** (Table 1), and thus titrations with bromide and iodide were omitted. The lower halide affinity of the thiophene-based receptors is ascribed to a weakened bidentate complexation caused by a more acute bite angle (vide infra).

**Isothermal Titration Calorimetry Studies.** To gain insights from an independent experimental technique and to understand the enthalpic and entropic contributions to the binding event, ITC measurements were performed for selected anion–receptor combinations.

As seen in the NMR titration experiments, a binding preference of **2a** for more charge-dense halides ( $\text{Cl}^- > \text{Br}^- > \text{I}^-$ ) was observed (Table 2). While the enthalpic contribution decreases from iodide to bromide to chloride, the entropic term, and as a net result the binding affinity, increases. Thus, the complexation appears to be driven by the liberation of solvent molecules for the smaller halides.<sup>77,78</sup> Notably, in the case of bromide and particularly for chloride, a significant amount of heat is still released after the addition of one equiv of halide, which requires the use of a TwoSites model for evaluation of the titration data (i.e., two complexation sites have to be taken into account) (Figure 4).<sup>79</sup> The stronger process ( $K_1 \approx 10^5 \text{ M}^{-1}$ ) is ascribed to the formation of a bidentate halogen bond with the anion, whereas the weaker process ( $K_2 \approx 10^3 \text{ M}^{-1}$ ) is tentatively assigned to monodentate halogen bonding. For both steps, a 1:1 stoichiometry ( $N_1 \approx 1, N_2 \approx 1$ ) is observed. In the case of iodide, the analysis was conducted with both models to ensure comparability; however, the OneSites model enables determination of the association constants with smaller errors (see Figures S52 and S53, SI). The bidentate complexation mode appears to be predominant for the larger iodide.

For bromo-substituted receptor **2b**, the OneSites model (see Figure S55, SI) is applicable and reveals a significantly weaker complexation. In line with the lower polarizability of the C–Br bond, this process is assigned to the formation of a bidentate halogen bond, whereas monodentate complexation is presumably too weak to be detected in this case. For hydrogen bond-based reference system **2**, no heat effect can be observed in the ITC measurement even at very high concentrations of host and guest.

The titration curve of thienyl-based system **3a** was fitted using the OneSites model (see Figure S56, SI). Considering the association constants found for **2a** and chloride, the complexation is interpreted as the formation of a monodentate halogen bond, which is plausible given that the two E–X bonds of **3a** are nearly parallel in the solid state (see Figures 1 and 5). The stoichiometry factor between one and two ( $N = 1.42$ ) indicates that both a 1:1 and a 1:2 complex are formed.<sup>34</sup>

Comparison of the chloride affinity of **2a** and **2b** with that of the corresponding imidazolium-based analogues ( $K_1 = 5.20 \times 10^5 \text{ M}^{-1}$ )<sup>34</sup> reveals a slightly lower halogen bond donor

strength for the 1,2,3-triazolium-based receptor, which is expected because fewer nitrogen atoms are positioned adjacent to the C–X bond (vide infra).<sup>29</sup>

**DFT Calculations.** The binding mode of the chloride complexes of **2a** and **3a** were investigated by quantum chemical calculations using density functional theory (DFT). As shown in Figure 5, the thienyl-based system exhibits a more acute bite angle ( $\alpha$ ), which precludes the formation of two short, linear halogen bonds with a single anion. As a consequence, a monodentate halogen bond with chloride is more stable, which enables the establishment of a second halogen bond (see the experimentally determined  $N$  value of 1.42, Table 2). Consistently, the association constants observed in the NMR and ITC studies for the thienyl-based hosts are lower than those in the phenyl-based systems. Prospectively, effective bidentate binding of larger, polyatomic anions might be achieved with **3a**.

To better understand the electronic influence of the electron-withdrawing group E on the C–X bond, DFT calculations were performed for related N-heterocyclic model systems (Figure 6). First, the positive charge induces a shift to a more positive electrostatic potential for the whole receptor, including the  $\sigma$  hole. Second, when comparing the iodo- and bromo-substituted receptors, a larger  $\sigma$  hole area is clearly visible in the receptor with the iodine atom, which is the result of enhanced E–X polarization. Consistently, lower anion affinities have been found experimentally for the bromo-substituted receptors (**2b** and **3b**). Furthermore, the DFT calculations show that the  $\sigma$  hole of halo-1,2,3-triazolium and halo-imidazolium are comparable, whereas the  $\sigma$  hole of the halo-1,2,4-triazolium is significantly larger (Figure 6). On the basis of the CH-acidities of 1,2,3-triazolium, imidazolium, and 1,2,4-triazolium ( $\text{p}K_{\text{a}} = 24, 20\text{--}23, \text{ and } 17\text{--}19$ , respectively),<sup>29</sup> it is obvious that C–X polarization increases with increasing nitrogen number and is particularly strong if the nitrogen atoms are placed adjacent to the C–X bond. Consequently, the halogen bond donor strength is expected to adopt the order halo-1,2,3-triazolium < halo-imidazolium < halo-1,2,4-triazolium. In agreement with this ordering, the imidazolium-based receptors exhibit anion affinities that are slightly enhanced compared to those of their 1,2,3-triazolium counterparts. The observed instability of the halo-1,2,4-triazolium salts (vide supra) can be rationalized by the excessive polarization of the C–X bond, leading to a substantial population of the  $\sigma^*(\text{E–X})$  orbital upon halogen bond formation and, thereby, to destabilization of the E–X bond.<sup>80–82</sup>

## CONCLUSION

A series of bidentate anion receptors based on halo-1,2,3-triazoliums featuring a 1,3-phenylene spacer was studied comprehensively by making use of two experimental techniques, namely, NMR spectroscopy and ITC titration experiments. The new receptors were readily synthesized via copper(I)-catalyzed azide–alkyne click chemistry, methylation, and formation of a silver(I) precursor. The latter was efficiently converted to the final halo-1,2,3-triazoliums by treatment with the corresponding halogens. The influence of different parameters on the anion affinities was investigated by comparison with selected reference systems. For a better understanding of the anion binding modes, several anion–receptor complexes were characterized by X-ray diffraction and modeled by means of DFT calculations. The following conclusions can be drawn from the collected data: (1) For

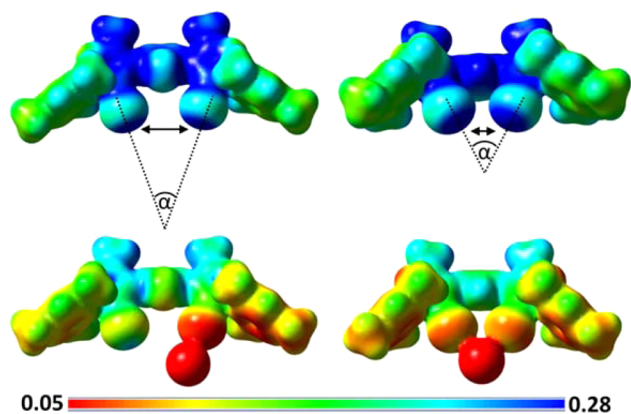


**Figure 5.** (Top) Calculated molecular electrostatic potential surface mapped on total density (isovalue 0.01) for **3a** (left) and **2a** (right) demonstrating the different bite angles ( $\alpha$ ) to the anion and the different distances between the halogen bond-donor atoms. (Bottom) **3a** (left) and **2a** (right) interacting with chloride.

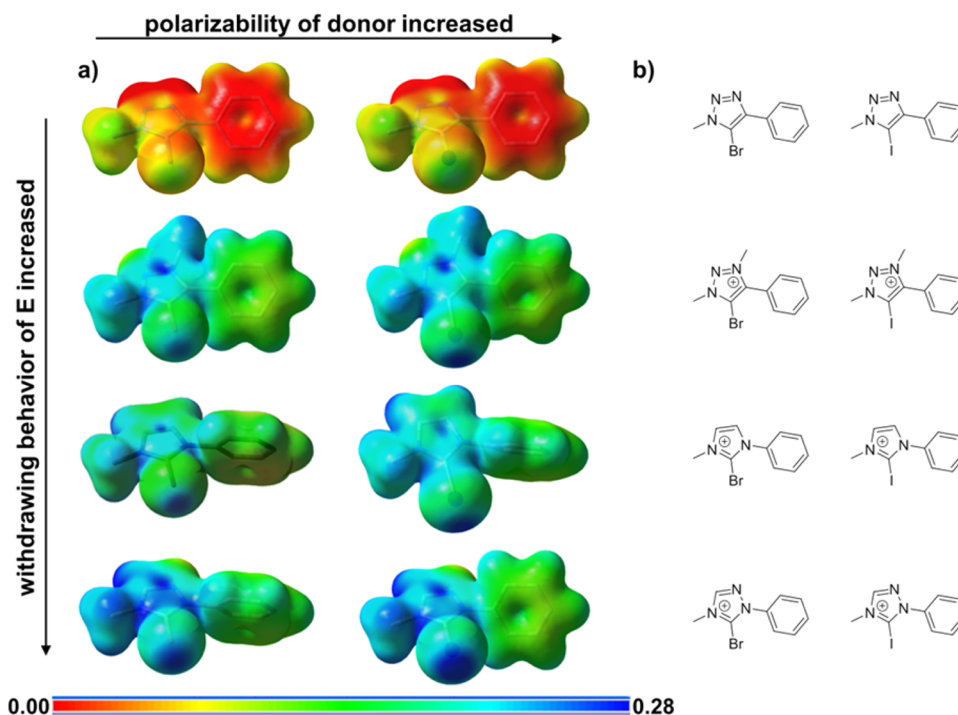


**Figure 6.** (a) Calculated molecular electrostatic potential surfaces mapped on total density (isovalue 0.01). Note that all electrostatic potential surfaces are plotted with the same parameters to warrant comparability. (b) Schematic representation of the corresponding chemical structures.

the iodo-1,2,3-triazolium-based receptor, which revealed the highest binding strength, the anion affinity increases in the order  $I^- < Br^- < Cl^- < AcO^- < H_2PO_4^{2-} < SO_4^{2-}$ . (2) When comparing analogous hydrogen bond- and halogen bond-based receptors, the latter shows a significantly higher association constant, which in turn is higher for iodine than for bromine as the bond donor atom. (3) The charge assistance and higher C–X polarization in the case of halo-1,2,3-triazolium-based receptors lead to a significantly higher anion affinity than for their halo-1,2,3-triazole counterparts. (4) The position of the nitrogen atoms within the triazolium ring substantially influences hydrogen/halogen bond donation. Relative to 1,2,3-triazoliums, the hydrogen bond strength for 1,2,4-triazolium-based receptors is higher. Unfortunately, the halo-1,2,4-triazolium analogues could not be isolated due to excessive C–X polarization. (5) Because of the strict linearity of the halogen bond angle, the utilized spacer unit exerts a pivotal influence on the binding mode, leading to a preference for monodentate halogen bonding for a thienyl spacer, which is in contrast to the favored bidentate configuration in the case of the phenyl bridge.

We believe that these conclusions provide essential information for the design of anion receptors based on N-heterocyclic halogen bond donors and will aid in the exploitation of their potential in anion sensing, anion templation, and organo-catalysis.

## EXPERIMENTAL SECTION

**General Experimental Methods.** All starting materials were purchased from commercially available sources and used as obtained unless otherwise specified. Mesityl azide,<sup>83</sup> 2,5-diethynylthiophene,<sup>84</sup> benzyl azide,<sup>85</sup> 1,3-bis(bromoethynyl)benzene,<sup>59</sup> 1,3-bis(1,2,4-triazol-1-yl)benzene,<sup>64</sup> 1,1'-(1,3-phenylene)bis(4-benzyl-1,2,4-triazol-4-ium) bromide,<sup>65</sup> 1,3-bis(1-benzyl-1H-1,2,3-triazol-4-yl)benzene,<sup>68</sup> 4,4'-(1,3-phenylene)bis(1-benzyl-3-methyl-1H-1,2,3-triazol-3-ium) tetrafluoroborate,<sup>69</sup> and silver(I)-oxide<sup>86</sup> were prepared according to literature

procedures. Silver(I)-oxide was stored in a desiccator in the dark. Tetrahydrofuran (THF) was dried and degassed with the help of a solvent purification system and kept under nitrogen using standard Schlenk techniques.  $CH_2Cl_2$  was dried by refluxing over calcium hydride and subsequent distillation under nitrogen. Ammonium tetrafluoroborate for the anion exchange was purchased in 99.999% purity. Most of the tetra-*n*-butylammonium anion salts for NMR and ITC analyses were ordered in high purity (>99%,  $(Bu_4N)AcO > 97%$ ), whereas  $(Bu_4N)_2SO_4$  was prepared from tetra-*n*-butylammonium hydroxide and sulfuric acid and stored in a desiccator *in vacuo*. MeCN and DMSO for ITC measurements were purchased in >99% purity (spectroscopic grade). NMR spectra were measured on spectrometer at 250, 300, 400, or 600 MHz in deuterated solvents at 25 °C. Chemical shifts were reported in ppm by using the solvent as an internal standard. Matrix-assisted laser desorption/ionization time-of-flight (MALDI-TOF) mass spectra (MS) were obtained using a TOF/TOF mass spectrometer with dithranol as the matrix. All spectra were measured in the positive-reflector mode using a Nd:YAG laser and a collision cell. Electrospray ionization (ESI)-MS spectra were measured on an ESI-(Q)-TOF-MS mass spectrometer equipped with an automatic syringe pump for sample injection. The mass spectrometer was operating in the positive-ion mode and the standard ESI source was used to generate the ions. Binding constants were obtained using WinEQNMR2<sup>73</sup> software in the case of NMR analysis and a MicroCal Origin 7.0-based software package in the case of ITC studies.

**Computational Details.** All calculations were performed with the Gaussian 09 (G09) program package<sup>87</sup> employing the DFT method using the M06-2X functional.<sup>88</sup> The iodine atom was treated by the 46-electron relativistic effective core potential MWB<sup>89</sup> for the inner shells, whereas the outer shells (i.e., 4s, 4p, 4d, and 5s electrons) were treated separately. The remaining atoms (i.e., C, H, N, and S) were treated with a basis set of quadruple- $\zeta$  valence quality.<sup>90</sup> The bulk solvent effects (MeCN) were included using the integral equation formalism of the polarizable continuum model by Tomasi and co-workers.<sup>91</sup> Geometry optimizations were performed without any constraints, and the true nature was confirmed by normal-mode analysis. Visualization of the electrostatic potential was performed using the GaussView 5.0 package.<sup>92</sup>



**Crystal Structure Determination.** The intensity data for the compounds were collected on a Nonius Kappa CCD diffractometer, using graphite-monochromated Mo  $K_{\alpha}$  radiation. Data were corrected for Lorentz and polarization effects; absorption was taken into account on a semiempirical basis using multiple scans.<sup>93–95</sup> The structures were solved by direct methods (SHELXS<sup>96</sup>) and refined by full-matrix least-squares techniques against  $F_o^2$  (SHELXL-97<sup>96</sup>). The hydrogen atoms bound to the compounds **1b**, **2a**-SO<sub>4</sub>, and 1,2,4-triazolium-5-oxide were located by difference Fourier synthesis and refined isotropically. All other hydrogen atoms were included at calculated positions with fixed thermal parameters. All non-hydrogen atoms were refined anisotropically.<sup>96</sup> The crystal of **1a** contains large voids that were filled with disordered solvent molecules. The size of the voids are 249 Å<sup>3</sup>/unit cell. Their contribution to the structure factors was secured by back-Fourier transformation using the SQUEEZE routine of the program PLATON<sup>97</sup> resulting in 32 electrons/unit cell. The crystals of 5-bromo-1,2,4-triazolium were extremely thin and of low quality, resulting in a substandard data set; however, the structure is sufficient to show connectivity and geometry despite the high final *R* value. We will only publish the conformation of the molecule and the crystallographic data but will not deposit the data in the Cambridge Crystallographic Data Centre. Crystallographic data as well as structure solution and refinement details are summarized in Tables S2 and S3 in the SI. MERCURY-3.3 was used for structure representations.

**Synthetic Procedures. General Procedure (A) for the CuAAC Reaction (Adopted from ref 98).** A 250 mL round-bottom flask was charged with an ethanol/water/CH<sub>2</sub>Cl<sub>2</sub> (2:1:1) mixture (100 mL) and purged with nitrogen. Successively, mesityl azide (2.4 equiv) or benzyl azide (3.0 equiv), copper(II) sulfate (0.2 equiv) dissolved in water (1 mL), sodium ascorbate (2 equiv) dissolved in water (6 mL), and 1,3-diethynylbenzene (1 equiv) or 2,5-diethynylthiophene (1 equiv) were added. Under the exclusion of light, the reaction mixture was stirred at 50 °C under a nitrogen atmosphere overnight, whereupon a precipitate was formed. After complete conversion was confirmed by TLC, 40 drops of *N*-(2-hydroxyethyl)ethylenediaminetriacetic acid (HEEDTA) were added, and the reaction mixture was stirred for 30 min at 50 °C. After cooling to room temperature, water (150 mL) was added, and the reaction mixture was extracted three times with CH<sub>2</sub>Cl<sub>2</sub>. The combined organic phases were washed with water, dried over sodium sulfate, filtered, and concentrated *in vacuo*. After precipitation by dropping the concentrated CH<sub>2</sub>Cl<sub>2</sub> solution into *n*-pentane, washing with *n*-pentane, and drying *in vacuo*, the product was obtained as a white or yellow solid.

**General Procedure (B) for Methylation with Meerwein's Salt (Adopted from refs 21 and 99).** A Schlenk flask was loaded with a bis-triazole derivative educt (1 equiv) dissolved in dry CH<sub>2</sub>Cl<sub>2</sub> (20 mL) and Meerwein's salt (trimethyloxonium tetrafluoroborate, 2.2 equiv), and the resulting mixture was stirred at room temperature under a nitrogen atmosphere until TLC-monitoring indicated full conversion of the educt (silica, CH<sub>2</sub>Cl<sub>2</sub>/MeOH (95:5)). After adding MeOH (2 mL) to quench excessive oxonium salt, the turbid reaction mixture became clear and was evaporated to dryness. The residue was dissolved in acetone or MeCN and precipitated by dropping the concentrated solution into diethyl ether. The precipitate was washed with diethyl ether and dried to yield the desired product.

**General Procedure (C) for Synthesis of the Silver(I) Precursors (Adopted from ref 99).** A Schlenk flask was charged with a bis-triazolium derivative educt (1 equiv), desiccator-dried Ag<sub>2</sub>O (3 equiv), and activated 3 Å molecular sieves.<sup>100</sup> Dry and degassed MeCN (20 mL) was added in the counterflow of nitrogen, and the reaction mixture was heated under reflux while being excluded from light for 12 h under nitrogen. After cooling to room temperature, the mixture was filtered over Celite with the help of MeCN as eluent. After being concentrated *in vacuo*, the crude product was purified by precipitation of the MeCN solution into diethyl ether. The resulting precipitate was filtered, washed with diethyl ether, and dried to yield the product as a white solid. The product was stored under nitrogen in a Schlenk flask in the fridge.

**General Procedure (D) for the Reaction of the Silver(I) Precursors with Halogens.** A Schlenk flask was loaded with the silver(I) precursor (1 equiv) dissolved in dry CH<sub>2</sub>Cl<sub>2</sub> (10 mL) for the phenyl-based receptors or in a dry CH<sub>2</sub>Cl<sub>2</sub>/MeCN (1:1) mixture for the thienyl-based receptors. Under the exclusion of light, the halogen (2.2 equiv) was added dropwise at 0 °C. Therefore, the amount of iodine was directly dissolved in dry and previously degassed MeCN (2 mL). In the case of bromine, a 0.66 M stock solution in dry CH<sub>2</sub>Cl<sub>2</sub> was prepared. After addition of the halogen, the reaction mixture was kept stirring at 0 °C for 30 min and then for 1 h at room temperature. The resulting suspension was dropped into diethyl ether to remove the excessive halogen, and the residue was filtered and washed with diethyl ether. After rinsing with MeCN and concentration of the filtrate *in vacuo*, the mixture was filtered over Celite with the help of MeCN as eluent to remove the remaining silver salt. The clear solution was evaporated to dryness; the resulting residue was dissolved in a CH<sub>2</sub>Cl<sub>2</sub>/MeOH (9:1) mixture and extracted five times with a 1 M aqueous ammonium tetrafluoroborate solution and two times with water (for a related anion exchange, see ref 101). After complete removal of the solvent *in vacuo*, the desired product was isolated and further purified by crystallization through vapor diffusion of diethyl ether into a concentrated solution of the product.

**1,3-Bis(1-mesityl-1H-1,2,3-triazol-4-yl)benzene (1).** Following general procedure A, mesityl azide (2.80 g, 17.4 mmol), copper(II) sulfate (230 mg, 1.44 mmol), sodium ascorbate (2.85 g, 14.4 mmol) and commercially available 1,3-diethynylbenzene (907 mg, 955 μL, 7.2 mmol) were allowed to react for 5 h at 50 °C and for 40 h at room temperature to yield desired product **1** as a white solid (3.08 g, 96%). <sup>1</sup>H NMR (250 MHz, CD<sub>2</sub>Cl<sub>2</sub>): δ 8.47 (s, 1H), 8.00 (s, 2H), 7.94 (dd, <sup>4</sup>*J* = 1.3 Hz, <sup>3</sup>*J* = 7.7 Hz, 2H), 7.57 (t, <sup>3</sup>*J* = 7.8 Hz, 1H), 7.05 (s, 4H), 2.38 (s, 6H), 2.02 (s, 12H). <sup>13</sup>C NMR (101 MHz, CD<sub>2</sub>Cl<sub>2</sub>): δ 147.6, 140.8, 135.6, 134.1, 132.0, 130.1, 129.6, 125.9, 123.4, 122.7, 21.4, 17.6. MS (MALDI-TOF, dithranol) *m/z*: 449.325 ([*M* + *H*]<sup>+</sup>). Anal. Calcd for C<sub>28</sub>H<sub>28</sub>N<sub>6</sub>: C, 74.97; H, 6.29; N, 18.74. Found: C, 74.68; H, 6.67; N, 18.52. Mp: 136–138 °C.

**1,3-Bis(5-iodo-1-mesityl-1H-1,2,3-triazol-4-yl)benzene (1a) (Adopted from refs 54 and 102).** The reaction was carried out in a two-neck Schlenk flask. The flask was equipped with an internal thermometer, and **1** (896 mg, 2.0 mmol) was added and dissolved in dry THF (18 mL). *n*-BuLi (2.5 M in hexane, 1.92 mL, 4.8 mmol, 2.4 equiv) was added dropwise over 30 min at approximately –78 °C; the solution changed color from yellow to dark red. After additional 10 min at –78 °C, iodine (1.32 g, 5.2 mmol, 2.6 equiv) dissolved in dry THF (5 mL) was added dropwise. The temperature was raised to room temperature within 1 h, and the mixture was stirred overnight. The mixture was washed with an aqueous sodium thiosulfate solution to quench the excess of iodine. The solution was extracted with CH<sub>2</sub>Cl<sub>2</sub> and the combined organic layers were washed with water. The organic phase was dried over sodium sulfate and filtered, and the solvent was removed. The crude product was purified by column chromatography (silica, 99:1 CH<sub>2</sub>Cl<sub>2</sub>/MeOH) to obtain the desired product **1a** in moderate yield (440 mg, 32%). Single crystals were obtained by slow vapor diffusion of *n*-pentane into a concentrated solution of **1a** in CH<sub>2</sub>Cl<sub>2</sub>. <sup>1</sup>H NMR (300 MHz, CD<sub>2</sub>Cl<sub>2</sub>): δ 8.83 (s, 1H), 8.18 (dd, <sup>4</sup>*J* = 1.6 Hz, <sup>3</sup>*J* = 7.8 Hz, 2H), 7.67 (t, <sup>3</sup>*J* = 7.8 Hz, 1H), 7.09 (s, 4H), 2.41 (s, 6H), 1.96 (s, 12H). <sup>13</sup>C NMR (63 MHz, CD<sub>2</sub>Cl<sub>2</sub>): δ 149.1, 140.9, 135.9, 133.0, 130.8, 129.1, 128.9, 127.2, 125.7, 79.8, 21.0, 17.2. MS (MALDI-TOF, dithranol) *m/z*: 701.049 ([*M* + *H*]<sup>+</sup>). Anal. Calcd for C<sub>28</sub>H<sub>26</sub>I<sub>2</sub>N<sub>6</sub>: C, 48.02; H, 3.74; I, 36.24; N, 12.00. Found: C, 48.32; H, 3.71; N, 11.85. Mp: 229–232 °C dec.

An alternative route is a copper(I)-catalyzed cycloaddition between 1,3-bis(iodoethynyl)benzene<sup>14</sup> and mesityl azide. A Schlenk flask was loaded with copper(I) iodide (115 mg, 0.60 mmol) and tris-(benzyltriazolylmethyl)amine (TBTA, 319 mg, 0.60 mmol) dissolved in dry THF (20 mL). This mixture was stirred for 3 h at room temperature and was then added to 1,3-bis(iodoethynyl)benzene (350 mg, 0.93 mmol) dissolved in 1 mL of dry THF. Subsequently, the mesityl azide (328 mg, 2.04 mmol) dissolved in 1 mL of dry THF was added slowly. The reaction mixture was stirred for 6 days at room temperature in the dark. 3 mL of 10% NH<sub>4</sub>OH solution were added to

the reaction mixture and, after removal of the solvent *in vacuo*, the remaining solid was dissolved in ethyl acetate, washed with water and brine, and concentrated *in vacuo*. The crude product was purified by column chromatography (silica, CH<sub>2</sub>Cl<sub>2</sub> to 95:5 CH<sub>2</sub>Cl<sub>2</sub>/diethyl ether) to obtain desired product **1a** in moderate yield (348 mg, 54%).

**1,3-Bis(5-bromo-1-mesityl-1H-1,2,3-triazol-4-yl)benzene (1b)** (Adopted from ref 56). A Schlenk flask was loaded with 1,3-bis(bromoethynyl)benzene (212 mg, 0.75 mmol) dissolved in dry THF (1.5 mL). Successively, mesityl azide (289 mg, 1.8 mmol, 2.4 equiv), copper(I) bromide (44 mg, 0.30 mmol, 20 mol % with respect to each bromoethynyl group), and copper(II) acetate (54 mg, 0.30 mmol, 20 mol % with respect to each bromoethynyl group) were added. The reaction mixture was stirred at 50 °C under nitrogen and TLC monitoring for a total of 2 weeks with additional dry THF added intermittently. Then, water was added and the solution was extracted three times with CH<sub>2</sub>Cl<sub>2</sub>. The combined organic layers were washed with an aqueous sodium hydrogen carbonate solution, brine, and twice with water. After removal of the solvent, the crude product was purified by column chromatography (silica, CH<sub>2</sub>Cl<sub>2</sub>) to obtain desired product **1b** in moderate yield (239 mg, 53%). Single crystals were obtained by slow vapor diffusion of *n*-pentane into a concentrated solution of **1b** in toluene. <sup>1</sup>H NMR (400 MHz, CD<sub>2</sub>Cl<sub>2</sub>): δ 8.87 (s, 1H), 8.20 (dd, <sup>4</sup>J = 1.6 Hz, <sup>3</sup>J = 7.8 Hz, 2H), 7.67 (t, <sup>3</sup>J = 7.8 Hz, 1H), 7.09 (s, 4H), 2.40 (s, 6H), 1.99 (s, 12H). <sup>13</sup>C NMR (101 MHz, CD<sub>2</sub>Cl<sub>2</sub>): δ 144.3, 141.6, 136.5, 132.2, 130.9, 129.7, 127.2, 125.0, 110.9, 21.5, 17.6. MS (MALDI-TOF, dithranol) *m/z*: 605.167 ([M + H]<sup>+</sup>). Anal. Calcd for C<sub>28</sub>H<sub>26</sub>Br<sub>2</sub>N<sub>6</sub>: C, 55.46; H, 4.32; Br, 26.36; N, 13.86. Found: C, 55.59; H, 4.33; N, 13.91. Mp: 187–189 °C.

**4,4'-(1,3-Phenylene)bis(5-iodo-1-mesityl-3-methyl-1H-1,2,3-triazolium) Tetrafluoroborate (2a)**. Following general procedure B, **1a** (300 mg, 0.43 mmol) and Meerwein's salt (139 mg, 0.94 mmol) were allowed to react for 64 h at room temperature. After purification, the desired product was precipitated by dropping the concentrated MeCN solution into diethyl ether (345 mg, 89%). Single crystals were obtained by dissolving **2a** in a MeCN/MeOH/diethyl ether mixture and storing it in the fridge for several weeks. <sup>1</sup>H NMR (250 MHz, acetone-*d*<sub>6</sub>): δ 8.48 (s, 1H), 8.29 (d, <sup>3</sup>J = 7.5 Hz, 2H), 8.13 (t, <sup>3</sup>J = 7.8 Hz, 1H), 7.29 (s, 4H), 4.59 (s, 6H), 2.44 (s, 6H), 2.13 (s, 12H). <sup>13</sup>C NMR (63 MHz, acetone-*d*<sub>6</sub>): δ 147.9, 144.1, 136.4, 135.1, 134.0, 132.4, 131.7, 130.7, 125.4, 93.9, 40.9, 21.2, 17.4. MS (MALDI-TOF, dithranol) *m/z*: 817.113 ([M - BF<sub>4</sub><sup>-</sup>]<sup>+</sup>). Anal. Calcd for C<sub>30</sub>H<sub>32</sub>B<sub>2</sub>F<sub>8</sub>I<sub>2</sub>N<sub>6</sub>: C, 39.86; H, 3.57; B, 2.39; F, 16.81; I, 28.08; N, 9.30. Found: C, 39.86; H, 3.55; N, 9.27. Mp: >280 °C dec.

**4,4'-(1,3-Phenylene)bis(1-mesityl-3-methyl-1H-1,2,3-triazolium) Tetrafluoroborate (2)**. Following general procedure B, **1** (896 mg, 2.0 mmol) and Meerwein's salt (651 mg, 4.4 mmol) were allowed to react for 64 h at room temperature. TLC monitoring indicated traces of the monomethylated side product; thus, additional Meerwein's salt (100 mg, 0.7 mmol) was added, and the mixture was stirred over another night. Desired product **2** was precipitated by dropping a concentrated acetone solution into diethyl ether (1.11 g, 86%). <sup>1</sup>H NMR (300 MHz, acetone-*d*<sub>6</sub>): δ 9.24 (s, 2H), 8.55 (s, 1H), 8.29 (d, <sup>3</sup>J = 7.8 Hz, 2H), 8.02 (t, <sup>3</sup>J = 7.8 Hz, 1H), 7.22 (s, 4H), 4.63 (s, 6H), 2.40 (s, 6H), 2.19 (s, 12H). <sup>13</sup>C NMR (63 MHz, acetone-*d*<sub>6</sub>): δ 143.9, 143.5, 135.9, 133.8, 132.7, 132.6, 132.4, 131.5, 130.7, 125.1, 40.2, 21.2, 17.3. HRMS (ESI-TOF) *m/z*: [M - BF<sub>4</sub><sup>-</sup>]<sup>+</sup> calcd for C<sub>30</sub>H<sub>34</sub>BF<sub>4</sub>N<sub>6</sub>, 565.2874; found, 565.2867. Anal. Calcd for C<sub>30</sub>H<sub>34</sub>B<sub>2</sub>F<sub>8</sub>N<sub>6</sub>·0.5H<sub>2</sub>O: C, 54.49; H, 5.34; B, 3.27; F, 22.98; N, 12.71; O, 1.21. Found: C, 54.34; H, 5.20; N, 12.75. Mp: 142–144 °C.

**4,4'-(1,3-Phenylene)bis(1-mesityl-3-methyl-1H-1,2,3-triazolium) silver Tetrafluoroborate (2Ag)**. Following general procedure C, **2** (652 mg, 1.0 mmol) and Ag<sub>2</sub>O (696 mg, 3.0 mmol) were allowed to react under reflux overnight to obtain **2Ag** in good yield (525 mg, 78%). <sup>1</sup>H NMR (250 MHz, CD<sub>3</sub>CN): δ 7.73–7.66 (m, 4H), 7.00 (s, 4H), 4.08 (s, 6H), 2.43 (s, 6H), 1.74 (s, 12H). <sup>13</sup>C NMR (75 MHz, CD<sub>3</sub>CN): δ 149.0, 141.5, 137.1, 135.1, 132.4, 131.8, 130.9, 130.7, 130.1, 129.3, 38.4, 21.4, 17.3.

**4,4'-(1,3-Phenylene)bis(5-bromo-1-mesityl-3-methyl-1H-1,2,3-triazolium) Tetrafluoroborate (2b)**. Following general procedure D, **2Ag** (201 mg, 0.3 mmol) dissolved in dry CH<sub>2</sub>Cl<sub>2</sub> (10 mL) was

reacted with 1 mL of a 0.66 M stock solution of bromine (104 mg, 0.66 mmol) in dry CH<sub>2</sub>Cl<sub>2</sub>. After removal of the silver salt and anion exchange, desired product **2b** was isolated in good yield as a white solid (208 mg, 86%). Single crystals with a bound bromide were obtained by slow vapor diffusion of diethyl ether into a concentrated solution of **2b** before anion exchange in a 9:1 MeCN/MeOH mixture. <sup>1</sup>H NMR (300 MHz, CD<sub>3</sub>CN): δ 8.23–8.01 (m, 4H), 7.26 (s, 4H), 4.39 (s, 6H), 2.43 (s, 6H), 2.14 (s, 12H). <sup>13</sup>C NMR (63 MHz, CD<sub>3</sub>CN): δ 144.8, 142.8, 136.4, 135.0, 133.1, 132.1, 131.0, 130.4, 123.9, 121.0, 41.5, 21.3, 17.4. MS (MALDI-TOF, dithranol) *m/z*: 721.201 ([M - BF<sub>4</sub><sup>-</sup>]<sup>+</sup>). Anal. Calcd for C<sub>30</sub>H<sub>32</sub>B<sub>2</sub>Br<sub>2</sub>F<sub>8</sub>N<sub>6</sub>: C, 44.48; H, 3.98; Br, 2.67; Br, 19.73; F, 18.76; N, 10.38. Found: C, 44.49; H, 4.38; N, 10.61. Mp: 241–243 °C.

**2,5-Bis(1-mesityl-1H-1,2,3-triazol-4-yl)thiophene (6)**. Following general procedure A, mesityl azide (2.90 g, 18.0 mmol), copper(II) sulfate (240 mg, 1.5 mmol), sodium ascorbate (2.97 g, 15 mmol), and 2,5-diethynylthiophene (991 mg, 7.5 mmol) were allowed to react for 17 h at 50 °C to yield **6** as a yellow solid (2.86 g, 84%). <sup>1</sup>H NMR (250 MHz, CDCl<sub>3</sub>): δ 7.79 (s, 2H), 7.49 (s, 2H), 7.02 (s, 4H), 2.37 (s, 6H), 2.04 (s, 12H). <sup>13</sup>C NMR (63 MHz, CDCl<sub>3</sub>): δ 142.4, 140.2, 135.1, 133.2, 132.4, 129.1, 124.8, 121.0, 21.1, 17.4. MS (MALDI-TOF, dithranol) *m/z*: 455.359 ([M + H]<sup>+</sup>). Anal. Calcd for C<sub>26</sub>H<sub>26</sub>N<sub>6</sub>S: C, 68.69; H, 5.76; N, 18.49; S, 7.05. Found: C, 68.57; H, 5.61; N, 18.31; S, 7.04. Mp: >280 °C dec.

**4,4'-(2,5-Thiophene)bis(1-mesityl-3-methyl-1H-1,2,3-triazolium) Tetrafluoroborate (3)**. Following general procedure B, **6** (910 mg, 2.0 mmol) and Meerwein's salt (651 mg, 4.4 mmol) were allowed to react for 23 h at room temperature. During purification, a concentrated acetone solution was dropped into diethyl ether, and the resulting precipitate was filtered, washed, and dried to yield **3** as a yellow solid (1.24 g, 94%). <sup>1</sup>H NMR (250 MHz, acetone-*d*<sub>6</sub>): δ 9.43 (s, 2H), 8.15 (s, 2H), 7.23 (s, 4H), 4.73 (s, 6H), 2.41 (s, 6H), 2.19 (s, 12H). <sup>13</sup>C NMR (63 MHz, acetone-*d*<sub>6</sub>): δ 143.5, 138.4, 135.8, 134.6, 132.4, 132.3, 130.6, 128.1, 40.6, 21.1, 17.2. MS (ESI-TOF) *m/z*: 571.241 ([M - BF<sub>4</sub><sup>-</sup>]<sup>+</sup>). Anal. Calcd for C<sub>28</sub>H<sub>32</sub>B<sub>2</sub>F<sub>8</sub>N<sub>6</sub>S: C, 51.09; H, 4.90; B, 3.28; F, 23.09; N, 12.77; S, 4.87. Found: C, 50.83; H, 5.04; N, 12.50; S, 4.61. Mp: >280 °C dec.

**4,4'-(2,5-Thiophene)bis(1-mesityl-3-methyl-1H-1,2,3-triazolium) silver Tetrafluoroborate (3Ag)**. Following general procedure C, **3** (658 mg, 1.0 mmol) and Ag<sub>2</sub>O (696 mg, 3.0 mmol) were heated to reflux overnight. After this time, <sup>1</sup>H NMR analysis showed ~20% conversion. Consequently, the mixture was stirred another day under heating to reflux to reach full conversion after 44 h. After the general purification, **3Ag** was isolated in good yield (524 mg, 78%). <sup>1</sup>H NMR (400 MHz, CD<sub>3</sub>CN): δ 7.63 (s, 2H), 7.08 (s, 4H), 4.34 (s, 6H), 2.38 (s, 6H), 1.70 (s, 12H). <sup>13</sup>C NMR (63 MHz, CD<sub>3</sub>CN): δ 169.2 (d, <sup>1</sup>J = 172.5 Hz, <sup>107/109</sup>Ag-<sup>13</sup>C), 142.8, 142.2, 137.0, 135.2, 131.3, 130.9, 130.3, 39.6, 21.2, 17.2.

**4,4'-(2,5-Thiophene)bis(5-iodo-1-mesityl-3-methyl-1H-1,2,3-triazolium) Tetrafluoroborate (3a)**. Following general procedure D, **3Ag** (203 mg, 0.3 mmol) dissolved in a 1:1 CH<sub>2</sub>Cl<sub>2</sub>/MeCN mixture (10 mL) was reacted with iodine (168 mg, 0.66 mmol) dissolved in MeCN (2 mL). After purification, **3a** was isolated in good yield as a green solid (243 mg, 89%). Single crystals were obtained by slow vapor diffusion of diethyl ether into a solution of **3a** in DMF. <sup>1</sup>H NMR (250 MHz, DMF-*d*<sub>7</sub>): δ 8.27 (s, 2H), 7.34 (s, 4H), 4.72 (s, 6H), 2.45 (s, 6H), 2.13 (s, 12H). <sup>13</sup>C NMR (75 MHz, DMF-*d*<sub>7</sub>): δ 144.1, 143.2, 136.5, 135.8, 132.6, 130.9, 129.0, 98.5, 41.3, 21.5, 17.6. HRMS (ESI-TOF) *m/z*: [M]<sup>2+</sup> calcd for C<sub>28</sub>H<sub>30</sub>I<sub>2</sub>N<sub>6</sub>S, 368.0166; found, 368.0187. Mp: 196–200 °C dec.

**4,4'-(2,5-Thiophene)bis(5-bromo-1-mesityl-3-methyl-1H-1,2,3-triazolium) Tetrafluoroborate (3b)**. Following general procedure D, **3Ag** (203 mg, 0.3 mmol) dissolved in a 1:1 CH<sub>2</sub>Cl<sub>2</sub>/MeCN mixture (10 mL) was reacted with 1 mL of a 0.66 M stock solution of bromine (104 mg, 0.66 mmol) in dry CH<sub>2</sub>Cl<sub>2</sub>. After removal of the silver salt and anion exchange, **3b** was isolated in good yield as a yellow solid (228 mg, 93%). Single crystals were obtained by slow vapor diffusion of diethyl ether into a concentrated solution of **3b** in MeCN. <sup>1</sup>H NMR (250 MHz, CD<sub>3</sub>CN): δ 8.01 (s, 2H), 7.26 (s, 4H), 4.47 (s, 6H), 2.43 (s, 6H), 2.12 (s, 12H). <sup>13</sup>C NMR (75 MHz, CD<sub>3</sub>CN): δ 144.9, 138.2,

136.5, 135.9, 131.0, 130.4, 127.3, 121.5, 41.9, 21.3, 17.5. MS (ESI-TOF)  $m/z$ : 727.060 ( $[M - BF_4^-]^+$ ). Anal. Calcd for  $C_{28}H_{30}B_2Br_2F_8N_6S$ : C, 41.21; H, 3.71; B, 2.65; Br, 19.58; F, 18.62; N, 10.30; S, 3.93. Found: C, 40.92; H, 3.67; N, 10.46; S, 3.67. Mp: 184–187 °C dec.

**1,1'-(1,3-Phenylene)bis(4-benzyl-1,2,4-triazol-4-ium) Tetrafluoroborate (4).** 1,1'-(1,3-Phenylene)bis(4-benzyl-1,2,4-triazol-4-ium) bromide (400 mg, 0.73 mmol) was dissolved in a 1:1 DMSO/MeOH mixture (10 mL) and slowly dropped into a 0.3 M aqueous ammonium tetrafluoroborate solution (150 mL). The precipitated white solid was filtered, washed with water, and dried to obtain **4** (390 mg, 94%).  $^1H$  NMR (300 MHz,  $CD_3CN$ ):  $\delta$  9.95 (s, 2H), 8.89 (s, 2H), 8.28 (s, 1H), 8.04 (d,  $^3J = 7.4$  Hz, 2H), 7.92 (t,  $^3J = 7.5$  Hz, 1H), 7.65–7.44 (m, 10H), 5.55 (s, 4H).  $^{13}C$  NMR (63 MHz,  $CD_3CN$ ):  $\delta$  145.9, 142.2, 137.2, 133.4, 132.8, 130.9, 130.6, 130.5, 124.3, 115.5, 53.3. MS (ESI-TOF)  $m/z$ : 481.214 ( $[M - BF_4^-]^+$ ). Anal. Calcd for  $C_{24}H_{22}B_2F_8N_6$ : C, 50.74; H, 3.90; B, 3.81; F, 26.75; N, 14.79. Found: C, 50.42; H, 4.16; N, 14.75. Mp: 262–264 °C.

**1,1'-(1,3-Phenylene)bis(4-benzyl-1,2,4-triazol-4-ium)silver Tetrafluoroborate (4Ag).** In this case, general procedure C had to be varied because of the second acidic hydrogen atom of the 1,2,4-triazolium. Consequently, **4** (89 mg, 0.16 mmol) and only 1 equiv of  $Ag_2O$  (36 mg, 0.16 mmol) in dry and degassed MeCN (5 mL) were allowed to react for 2.5 h under reflux to obtain the desired product **4Ag** in good yield after the general purification steps (81 mg, 88%).  $^1H$  NMR (300 MHz,  $CD_3CN$ ):  $\delta$  8.64 (s, 2H), 8.09–7.89 (m, 3H), 7.75 (t,  $^3J = 8.4$  Hz, 1H), 7.03–6.62 (m, 10H), 5.07 (s, 4H).  $^{13}C$  NMR (101 MHz,  $CD_3CN$ ):  $\delta$  180.1 (d,  $^1J = 199.0$  Hz,  $^{107/109}Ag-^{13}C$ ), 146.0, 140.5, 136.1, 132.7, 129.7, 129.6, 129.4, 123.6, 113.0, 53.4.

## ■ ASSOCIATED CONTENT

### ■ Supporting Information

NMR spectra, binding studies, X-ray data, and DFT calculation data. This material is available free of charge via the Internet at <http://pubs.acs.org>. Crystallographic data (excluding structure factors) have been deposited with the Cambridge Crystallographic Data Centre as supplementary publication CCDC-1022784 (**1a**), CCDC-1022785 (**1b**), CCDC-1022786 (**2a**), CCDC-1022787 (**2a-SO<sub>4</sub>**), CCDC-1022788 (**2b**), CCDC-1022789 (**3a**), and CCDC-1022790 (1,2,4-triazolium-5-oxide). Copies of the data can be obtained free of charge upon application to the CCDC at 12 Union Road, Cambridge CB2 1EZ, U.K. E-mail: [deposit@ccdc.cam.ac.uk](mailto:deposit@ccdc.cam.ac.uk).

## ■ AUTHOR INFORMATION

### Corresponding Author

\*E-mail: [ulrich.schubert@uni-jena.de](mailto:ulrich.schubert@uni-jena.de).

### Notes

The authors declare no competing financial interest.

## ■ ACKNOWLEDGMENTS

R.T. is grateful for a scholarship from the Federal Ministry of Education and Research (“Deutschlandstipendium”). We also thank W. Günther and G. Sentsis (NMR spectroscopy) as well as E. Altuntas, N. Fritz, and S. Crotty (MALDI and ESI-MS) for discussions and performing experiments.

## ■ REFERENCES

- Albelda, M. T.; Frías, J. C.; García-España, E.; Schneider, H.-J. *Chem. Soc. Rev.* **2012**, *41*, 3859.
- Beer, P. D.; Gale, P. A. *Angew. Chem., Int. Ed.* **2001**, *40*, 486.
- Lehn, J.-M. *Science* **1993**, *260*, 1762.
- Kubik, S.; Reyheller, C.; Stüwe, S. *J. Inclusion Phenom. Macroyclic Chem.* **2005**, *52*, 137.

(5) Desiraju, G. R.; Ho, P. S.; Kloo, L.; Legon, A. C.; Marquardt, R.; Metrangolo, P.; Politzer, P.; Resnati, G.; Rissanen, K. *Pure Appl. Chem.* **2013**, *85*, 1711.

(6) Metrangolo, P.; Meyer, F.; Pilati, T.; Resnati, G.; Terraneo, G. *Angew. Chem., Int. Ed.* **2008**, *47*, 6114.

(7) Metrangolo, P.; Resnati, G. *Science* **2008**, *321*, 918.

(8) Caballero, A.; Zapata, F.; White, N. G.; Costa, P. J.; Félix, V.; Beer, P. D. *Angew. Chem., Int. Ed.* **2012**, *51*, 1876.

(9) Zapata, F.; Caballero, A.; White, N. G.; Claridge, T. D. W.; Costa, P. J.; Félix, V.; Beer, P. D. *J. Am. Chem. Soc.* **2012**, *134*, 11533.

(10) Asmus, S.; Beckendorf, S.; Zurro, M.; Mück-Lichtenfeld, C.; Fröhlich, R.; García Mancheño, O. *Chem.—Asian J.* **2014**, *9*, 2178.

(11) Beckendorf, S.; Asmus, S.; Mück-Lichtenfeld, C.; García Mancheño, O. *Chem.—Eur. J.* **2012**, *19*, 1581.

(12) Jungbauer, S. H.; Schindler, S.; Kniep, F.; Walter, S. M.; Rout, L.; Huber, S. M. *Synlett* **2013**, *24*, 2624.

(13) Walter, S. M.; Kniep, F.; Herdtweck, E.; Huber, S. M. *Angew. Chem., Int. Ed.* **2011**, *50*, 7187.

(14) Kniep, F.; Rout, L.; Walter, S. M.; Bensch, H. K. V.; Jungbauer, S. H.; Herdtweck, E.; Huber, S. M. *Chem. Commun. (Cambridge, U.K.)* **2012**, *48*, 9299.

(15) Kniep, F.; Walter, S. M.; Herdtweck, E.; Huber, S. M. *Chem.—Eur. J.* **2012**, *18*, 1306.

(16) Bruckmann, A.; Pena, M. A.; Bolm, C. *Synlett* **2008**, 900.

(17) Castelli, R.; Schindler, S.; Walter, S. M.; Kniep, F.; Overkleeft, H. S.; Van der Marel, G. A.; Huber, S. M.; Codée, J. D. C. *Chem.—Asian J.* **2014**, *9*, 2095.

(18) He, W.; Ge, Y.-C.; Tan, C.-H. *Org. Lett.* **2014**, *16*, 3244.

(19) Zurro, M.; Asmus, S.; Beckendorf, S.; Mück-Lichtenfeld, C.; García Mancheño, O. *J. Am. Chem. Soc.* **2014**, *136*, 13999.

(20) Ohmatsu, K.; Kiyokawa, M.; Ooi, T. *J. Am. Chem. Soc.* **2011**, *133*, 1307.

(21) Kilah, N. L.; Wise, M. D.; Serpell, C. J.; Thompson, A. L.; White, N. G.; Christensen, K. E.; Beer, P. D. *J. Am. Chem. Soc.* **2010**, *132*, 11893.

(22) Gilday, L. C.; Lang, T.; Caballero, A.; Costa, P. J.; Félix, V.; Beer, P. D. *Angew. Chem., Int. Ed.* **2013**, *52*, 4356.

(23) Mullaney, B. R.; Thompson, A. L.; Beer, P. D. *Angew. Chem., Int. Ed.* **2014**, *53*, 11458.

(24) Caballero, A.; Swan, L.; Zapata, F.; Beer, P. D. *Angew. Chem., Int. Ed.* **2014**, *53*, 11854.

(25) Mullaney, B. R.; Partridge, B. E.; Beer, P. D. *Chem.—Eur. J.* **2015**, *21*, 1660.

(26) Robinson, S. W.; Mustoe, C. L.; White, N. G.; Brown, A.; Thompson, A. L.; Kennepohl, P.; Beer, P. D. *J. Am. Chem. Soc.* **2015**, *137*, 499.

(27) Clark, T.; Hennemann, M.; Murray, J. S.; Politzer, P. *J. Mol. Model.* **2007**, *13*, 291.

(28) Erdelyi, M. *Chem. Soc. Rev.* **2012**, *41*, 3547.

(29) Schulze, B.; Schubert, U. S. *Chem. Soc. Rev.* **2014**, *43*, 2522.

(30) Politzer, P.; Lane, P.; Concha, M. C.; Ma, Y.; Murray, J. S. *J. Mol. Model.* **2007**, *13*, 305.

(31) Chudzinski, M. G.; McClary, C. A.; Taylor, M. S. *J. Am. Chem. Soc.* **2011**, *133*, 10559.

(32) Kilah, N. L.; Wise, M. D.; Beer, P. D. *Cryst. Growth Des.* **2011**, *11*, 4565.

(33) Beale, T. M.; Chudzinski, M. G.; Sarwar, M. G.; Taylor, M. S. *Chem. Soc. Rev.* **2013**, *42*, 1667.

(34) Walter, S. M.; Kniep, F.; Rout, L.; Schmidtchen, F. P.; Herdtweck, E.; Huber, S. M. *J. Am. Chem. Soc.* **2012**, *134*, 8507.

(35) Zapata, F.; Caballero, A.; Molina, P.; Alkorta, I.; Elguero, J. *J. Org. Chem.* **2014**, *79*, 6959.

(36) Caballero, A.; White, N. G.; Beer, P. D. *Angew. Chem., Int. Ed.* **2011**, *50*, 1845.

(37) Sarwar, M. G.; Dragisic, B.; Dimitrijević, E.; Taylor, M. S. *Chem.—Eur. J.* **2013**, *19*, 2050.

(38) Kniep, F.; Jungbauer, S. H.; Zhang, Q.; Walter, S. M.; Schindler, S.; Schnapperelle, I.; Herdtweck, E.; Huber, S. M. *Angew. Chem., Int. Ed.* **2013**, *52*, 7028.

- (39) Sarwar, M. G.; Dragisic, B.; Salsberg, L. J.; Gouliaras, C.; Taylor, M. S. *J. Am. Chem. Soc.* **2010**, *132*, 1646.
- (40) Mele, A.; Metrangolo, P.; Neukirch, H.; Pilati, T.; Resnati, G. *J. Am. Chem. Soc.* **2005**, *127*, 14972.
- (41) Sarwar, M. G.; Dragisic, B.; Sagoo, S.; Taylor, M. S. *Angew. Chem., Int. Ed.* **2010**, *49*, 1674.
- (42) Dimitrijević, E.; Kvak, O.; Taylor, M. S. *Chem. Commun. (Cambridge, U.K.)* **2010**, *46*, 9025.
- (43) Cametti, M.; Raatikainen, K.; Metrangolo, P.; Pilati, T.; Terraneo, G.; Resnati, G. *Org. Biomol. Chem.* **2012**, *10*, 1329.
- (44) Serpell, C. J.; Kilah, N. L.; Costa, P. J.; Félix, V.; Beer, P. D. *Angew. Chem., Int. Ed.* **2010**, *49*, 5322.
- (45) Gilday, L. C.; White, N. G.; Beer, P. D. *Dalton Trans.* **2013**, *42*, 15766.
- (46) Mercurio, J. M.; Knighton, R. C.; Cookson, J.; Beer, P. D. *Chem.—Eur. J.* **2014**, *20*, 11740.
- (47) Meldal, M.; Tornøe, C. W. *Chem. Rev.* **2008**, *108*, 2952.
- (48) Hein, J. E.; Fokin, V. V. *Chem. Soc. Rev.* **2010**, *39*, 1302.
- (49) Tornøe, C. W.; Christensen, C.; Meldal, M. *J. Org. Chem.* **2002**, *67*, 3057.
- (50) Rostovtsev, V. V.; Green, L. G.; Fokin, V. V.; Sharpless, K. B. *Angew. Chem., Int. Ed.* **2002**, *41*, 2596.
- (51) Juriček, M.; Kouwer, P. H. J.; Rowan, A. E. *Chem. Commun. (Cambridge, U.K.)* **2011**, *47*, 8740.
- (52) Lee, S.; Hua, Y.; Park, H.; Flood, A. H. *Org. Lett.* **2010**, *12*, 2100.
- (53) Schulze, B.; Friebe, C.; Hager, M. D.; Günther, W.; Köhn, U.; Jahn, B. O.; Görls, H.; Schubert, U. S. *Org. Lett.* **2010**, *12*, 2710.
- (54) Uhlmann, P.; Felding, J.; Vedso, P.; Begtrup, M. *J. Org. Chem.* **1997**, *62*, 9177.
- (55) Brotherton, W. S.; Clark, R. J.; Zhu, L. *J. Org. Chem.* **2012**, *77*, 6443.
- (56) Kuijpers, B. H. M.; Dijkmans, G. C. T.; Groothuys, S.; Quaedflieg, P. J. L. M.; Blaauw, R. H.; van Delft, F. L.; Rutjes, F. P. J. T. *Synlett* **2005**, 3059.
- (57) Hein, J. E.; Tripp, J. C.; Krasnova, L. B.; Sharpless, K. B.; Fokin, V. V. *Angew. Chem., Int. Ed.* **2009**, *48*, 8018.
- (58) Juriček, M.; Stout, K.; Kouwer, P. H. J.; Rowan, A. E. *Org. Lett.* **2011**, *13*, 3494.
- (59) Shu, L.; Müri, M.; Krupke, R.; Mayor, M. *Org. Biomol. Chem.* **2009**, *7*, 1081.
- (60) Mullen, K. M.; Mercurio, J.; Serpell, C. J.; Beer, P. D. *Angew. Chem., Int. Ed.* **2009**, *48*, 4781.
- (61) Donnelly, K. F.; Petronilho, A.; Albrecht, M. *Chem. Commun. (Cambridge, U.K.)* **2013**, *49*, 1145.
- (62) Mathew, P.; Neels, A.; Albrecht, M. *J. Am. Chem. Soc.* **2008**, *130*, 13534.
- (63) Saravanakumar, R.; Ramkumar, V.; Sankararaman, S. *Organometallics* **2011**, *30*, 1689.
- (64) Clark, W. D.; Tyson, G. E.; Hollis, T. K.; Valle, H. U.; Valente, E. J.; Oliver, A. G.; Dukes, M. P. *Dalton Trans.* **2013**, *42*, 7338.
- (65) Hollis, T.; Zhang, X. Air-stable, blue light emitting chemical compounds. WO 2011050003 A2, 2011.
- (66) Petronilho, A.; Müller-Bunz, H.; Albrecht, M. *Chem. Commun. (Cambridge, U.K.)* **2012**, *48*, 6499.
- (67) Caballero, A.; Bennett, S.; Serpell, C. J.; Beer, P. D. *CrystEngComm* **2013**, *15*, 3076.
- (68) Gower, M. L.; Crowley, J. D. *Dalton Trans.* **2010**, *39*, 2371.
- (69) Kilpin, K. J.; Paul, U. S. D.; Lee, A.-L.; Crowley, J. D. *Chem. Commun. (Cambridge, U.K.)* **2011**, *47*, 328.
- (70) Bondi, A. *J. Phys. Chem.* **1964**, *68*, 441.
- (71) Rosokha, S. V.; Stern, C. L.; Ritzert, J. T. *Chem.—Eur. J.* **2013**, *19*, 8774.
- (72) White, N. G.; Caballero, A.; Beer, P. D. *CrystEngComm* **2014**, *16*, 3722.
- (73) Hynes, M. J. *J. Chem. Soc., Dalton Trans.* **1993**, 311.
- (74) Caballero, A.; Zapata, F.; González, L.; Molina, P.; Alkorta, I.; Elguero, J. *Chem. Commun. (Cambridge, U.K.)* **2014**, *50*, 4680.
- (75) The chemical-shift migration of the 3,5-protons of the mesityl rings ( $H-3,5^{\text{mes}}$ ) was used for the determination of the binding constants because these signals are present in both phenyl- and thienyl-containing receptors and because the proton resonances for the central phenyl ring overlapped in the oxo-anion binding studies. Note that the analysis based on the chemical shifts of the triazolium protons ( $H-5^{\text{tr}}$ , see Table 1) and the protons of the triazolium's methyl group ( $\text{CH}_3-3^{\text{tr}}$ ) gave very similar results.
- (76) White, N. G.; Carvalho, S.; Félix, V.; Beer, P. D. *Org. Biomol. Chem.* **2012**, *10*, 6951.
- (77) Ursu, A.; Schmidtchen, F. P. *Angew. Chem., Int. Ed.* **2012**, *51*, 242.
- (78) Schmidtchen, F. P. *Chem. Soc. Rev.* **2010**, *39*, 3916.
- (79) Note that the SequentialBinding model, which implies a successive 1:1 and 1:2 complex formation, is not applicable here (see Figure S54, SI).
- (80) Hill, J. G.; Hu, X. *Chem.—Eur. J.* **2013**, *19*, 3620.
- (81) Legon, A. C. *Angew. Chem., Int. Ed.* **1999**, *38*, 2686.
- (82) Metrangolo, P.; Neukirch, H.; Pilati, T.; Resnati, G. *Acc. Chem. Res.* **2005**, *38*, 386.
- (83) Hu, H.; Zhang, A.; Ding, L.; Lei, X.; Zhang, L. *Molecules* **2008**, *13*, 556.
- (84) Neenan, T. X.; Whitesides, G. M. *J. Org. Chem.* **1988**, *53*, 2489.
- (85) Ju, Y.; Kumar, D.; Varma, R. S. *J. Org. Chem.* **2006**, *71*, 6697.
- (86) Huang, W.; Zhang, R.; Zou, G.; Tang, J.; Sun, J. *J. Organomet. Chem.* **2007**, *692*, 3804.
- (87) Frisch, M. J.; Trucks, G. W.; Schlegel, H. B.; Scuseria, G. E.; Robb, M. A.; Cheeseman, J. R.; Scalmani, G.; Barone, V.; Mennucci, B.; Petersson, G. A.; Nakatsuji, H.; Caricato, M.; Li, X.; Hratchian, H. P.; Izmaylov, A. F.; Bloino, J.; Zheng, G.; Sonnenberg, J. L.; Hada, M.; Ehara, M.; Toyota, K.; Fukuda, R.; Hasegawa, J.; Ishida, M.; Nakajima, T.; Honda, Y.; Kitao, O.; Nakai, H.; Vreven, T.; Montgomery, J. A., Jr.; Peralta, J. E.; Ogliaro, F.; Bearpark, M.; Heyd, J. J.; Brothers, E.; Kudin, K. N.; Staroverov, V. N.; Kobayashi, R.; Normand, J.; Raghavachari, K.; Rendell, A.; Burant, J. C.; Iyengar, S. S.; Tomasi, J.; Cossi, M.; Rega, N.; Millam, J. M.; Klene, M.; Knox, J. E.; Cross, J. B.; Bakken, V.; Adamo, C.; Jaramillo, J.; Gomperts, R.; Stratmann, R. E.; Yazyev, O.; Austin, A. J.; Cammi, R.; Pomelli, C.; Ochterski, J. W.; Martin, R. L.; Morokuma, K.; Zakrzewski, V. G.; Voth, G. A.; Salvador, P.; Dannenberg, J. J.; Dapprich, S.; Daniels, A. D.; Farkas, O.; Foresman, J. B.; Ortiz, J. V.; Cioslowski, J.; Fox, D. J. *Gaussian 09*, revision A.02; Gaussian, Inc.: Wallingford, CT, 2009.
- (88) Zhao, Y.; Truhlar, D. *Theor. Chem. Acc.* **2008**, *120*, 215.
- (89) Andrae, D.; Häußermann, U.; Dolg, M.; Stoll, H.; Preuß, H. *Theor. Chim. Acta* **1990**, *77*, 123.
- (90) Weigend, F.; Ahlrichs, R. *Phys. Chem. Chem. Phys.* **2005**, *7*, 3297.
- (91) Tomasi, J.; Mennucci, B.; Cammi, R. *Chem. Rev.* **2005**, *105*, 2999.
- (92) Dennington, R.; Keith, T.; Millan, J. *GaussView 5.0*, version 5.0.8; Semicchem, Inc.: Shawnee Mission, KS, 2009.
- (93) Nonius, B. V.; COLLECT; Netherlands, 1998.
- (94) Otwinowski, Z.; Minor, W. In *Methods in Enzymology*; Carter, C. W., Jr., Ed.; Academic Press: New York, 1997; Vol. 276, p 307.
- (95) Sheldrick, G. M.; SADABS, version 2.10, Bruker-AXS, Inc.: Madison, WI, 2002.
- (96) Sheldrick, G. *Acta Crystallogr. A* **2008**, *A64*, 112.
- (97) Spek, A. L. *Acta Crystallogr. D* **2009**, *D65*, 148.
- (98) Schulze, B.; Escudero, D.; Friebe, C.; Siebert, R.; Görls, H.; Sinn, S.; Thomas, M.; Mai, S.; Popp, J.; Dietzek, B.; González, L.; Schubert, U. S. *Chem.—Eur. J.* **2012**, *18*, 4010.
- (99) Schulze, B.; Escudero, D.; Friebe, C.; Siebert, R.; Görls, H.; Köhn, U.; Altuntas, E.; Baumgaertel, A.; Hager, M. D.; Winter, A.; Dietzek, B.; Popp, J.; González, L.; Schubert, U. S. *Chem.—Eur. J.* **2011**, *17*, 5494.
- (100) O, W. W. N.; Lough, A. J.; Morris, R. H. *Organometallics* **2009**, *28*, 853.
- (101) Hancock, L. M.; Gilday, L. C.; Kilah, N. L.; Serpell, C. J.; Beer, P. D. *Chem. Commun. (Cambridge, U.K.)* **2011**, *47*, 1725.
- (102) Satake, A.; Shoji, O.; Kobuke, Y. *J. Organomet. Chem.* **2007**, *692*, 635.